**AALBORG UNIVERSITY**

DENMARK

# DFT based spatial multiplexing and maximum ratio transmission for mm-wawe large MIMO

Phan-Huy, D.-T.; Tölli, A.; Rajatheva, N.; Carvalho, Elisabeth De

[Link to publication from Aalborg University](Link to publication from Aalborg University)

# DFT based spatial multiplexing and maximum ratio transmission for mm-wave large MIMO

D.-T. Phan-Huy*,
*Orange Labs, France
dinhthuy.phanhuy@orange.com

A. Tölli**, N. Rajatheva**,
** University of Oulu, Finland
antti.tolli@ee.oulu.fi, rrajathe@ee.oulu.fi

E. De Carvalho†,
†Aalborg University, Denmark
edc@es.aau.dk

*Abstract*—**By using large point-to-point multiple input multiple output (MIMO), spatial multiplexing of a large number of data streams in wireless communications using millimeter-waves (mm-waves) can be achieved. However, according to the antenna spacing and transmitter-receiver distance, the MIMO channel is likely to be ill-conditioned. In such conditions, highly complex schemes such as the singular value decomposition (SVD) are necessary. In this paper, we propose a new low complexity system called discrete Fourier transform based spatial multiplexing (DFT-SM) with maximum ratio transmission (DFT-SM-MRT). When the DFT-SM scheme alone is used, the data streams are either mapped onto different angles of departures in the case of aligned linear arrays, or mapped onto different orbital angular momentums in the case of aligned circular arrays. Maximum ratio transmission pre-equalizes the channel and compensates for arrays misalignments. Simulation results show that, although the DFT-SM-MRT scheme has a much lower complexity than the SVD scheme, it still achieves large spectral efficiencies and is robust to misalignment and reflection.**

*Keywords-component: Spatial multiplexing, precoder, DFT, maximum ratio transmission, large MIMO, millimeter-wave, orbital angular momentum, misalignment, 5G.*

## I. INTRODUCTION

An air interface such as the 60GHz WIFI standard [1-3], can provide throughputs of several Gigabits per second in indoor, by using millimeter-waves (mm-waves). Recent investigations, as illustrated by Fig. 1, propose to extend the use of mm-waves to the outdoor mesh networks [4-6] or to 5G networks [7], for both the direct link and the backhaul link.
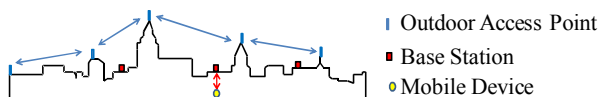


Fig. 1. Example of outdoor wireless meshed network

The well known multiple input multiple output (MIMO) spatial multiplexing techniques, enable to improve the spectral efficiency of a wireless link, by using several antennas at the transmitter and the receiver, provided that the rank of the MIMO channel is large enough [8]. For millimeter waves, a rank much higher than 1 can be achieved even in line-of-sight (LOS) conditions, as long as the spacing between antennas of the same array is chosen large enough compared to the transmitter-receiver distance (which is typically of tens to a few hundreds of meters) and the wavelength. For instance, in [1][9],

the diffraction theory in optics is used to compute the inter-antenna spacing which ensures that the angular separability of antennas of the transmit array and the angular resolution of the receiver array are equal. The computed inter-antenna spacing is a function of the distance between the transmitter and receiver and of the wavelength. It ensures that the MIMO channel is well conditioned. It thus allows the use of low complexity spatial multiplexing schemes such as the zero forcing (ZF) [10], the minimum mean square error (MMSE) [11] or the maximum ratio transmission (MRT)[12] precoders. Similar observations have been made in [13] for short-range communications exploiting the spherical wave.

One could extend the approach of [9] to the mm-waves and the large MIMO systems, which exploit hundreds of antennas to reach huge energy savings [14]. However, in practice, it seems difficult to deploy arrays with the inter-antenna spacing optimized for each possible distance between transmitters and receivers, and for each carrier frequency. If, contrary to what is shown in [9], the inter-antenna spacing is arbitrarily chosen, then the MIMO channel has a great risk to be ill conditioned. Singular value decomposition could be applied [15,16] to determine the number of data streams to be sent, assuming that channel state information are available both at the transmitter (CSIT) and the receiver (CSIR). However, in large MIMO systems, the complexity of the processing rapidly grows with the number of antennas, at both the receiver and the transceiver [14]. We acknowledge that for backhauling in the outdoor, the complexity is not an issue, because the channel is static or slowly varies. Indeed, in this case, the SVD processing can be done with a slow update rate. However, in cellular networks [7], where a frequent and fast update is required, low complexity schemes are preferable.

In this paper, we propose a new low complexity system for large MIMO mm-wave communications, with arbitrary inter-antenna spacing. This technique, called Discrete Fourier Transform based spatial multiplexing with maximum ratio transmission (DFT-SM-MRT) combines two techniques:

- DFT based Spatial Multiplexing (DFT-SM) ;
- MRT beamforming.

The DFT-SM scheme uses an inverse Discrete Fourier Transform (IDFT) performed in the spatial domain [17,18] at the transmitter, and a Discrete Fourier Transform (DFT) also in the spatial domain, at the receiver. When the DFT-SM scheme is used with linear arrays, the data streams are mapped onto

beams of various angles of departures [17,18] which are then detected at the receiver side, by beams with various angles of arrivals. When the DFT-SM scheme is used with circular arrays, data streams are mapped onto vortices with various orbital angular momentums [19]. The DFT-SM scheme is better suited for arrays being aligned according to Fig. 2 and Fig. 3, for linear and circular arrays, respectively. The authors of [18] have in fact demonstrated that the DFT-SM achieves the SVD performance, if the circular arrays are perfectly aligned. Also, based on a spherical wave channel model, [13] has shown that the alignment of linear arrays provide better conditions for spatial multiplexing in LOS conditions. In practice, slight misalignments (which are expected to reduce the number of streams which can be spatially multiplexed) cannot be avoided. We therefore introduce the MRT precoder based on CSIT, in order to pre-equalize the channel [11] and compensate for misalignments.



Fig. 2. DFT-SM for aligned linear arrays



Fig. 3. DFT-SM for aligned circular arrays

This paper is organized as follows. Section II introduces the common system model, section III presents the SVD, DFT-SM, DFT-SM-MRT schemes and a fourth scheme called "DFT-SM-MRT filtered". Section IV presents the performance evaluation methodology. Section V presents some numerical results and section VI concludes this paper. The following notations are used throughout this paper: $A^H$ is the transpose conjugate of A. $E[|.|^2]$ is the expectation operation. $A^{DFT}$ and $A^{IDFT}$ are the butler matrices corresponding to the DFT and IDFT operation respectively [21,22].

## II. COMMON SYSTEM MODEL

### A. System Description

A wireless link between a transmitter and a receiver, both having an identical array of $N$ antennas, is considered. In this paper, we restrict our analysis to a narrowband single carrier transmission, and we therefore consider the channel as being flat in the frequency domain. The results of the paper could easily be extended to the wideband multi-carrier scenario, by considering each sub-carrier, independently. Indeed, the 60GHz WIFI standard is based on orthogonal frequency division multiplex (OFDM) [1-3].

Assuming flat fading, one can model the MIMO propagation channel by a complex $N \times N$ matrix H. The Time division duplex (TDD) mode is considered, and CSIT and CSIR are assumed to be perfectly known. The transmitter sends a vector $a$ of $N$ complex data symbols with an average power $P_{data} = E[\frac{1}{N}\sum_{n=0}^{N-1}|a_n|^2]$. The power is equally shared between data streams. The transmitter multiplexes data streams by multiplying to the vector $a$ with the precoding matrix $\rho P$,

where $\rho$ is a normalizing factor ensuring that $\sum_{n=0}^{N-1}\sum_{p=0}^{N-1}|\rho P_{np}|^2 = 1$. The receiver de-multiplexes the data streams by applying the decoding matrix $\gamma Q$, with $\gamma$ being a normalizing factor ensuring that $\sum_{p=0}^{N-1}|\gamma Q_{np}|^2 = 1, \forall n$. Let $w$ be the vector of the additive white Gaussian noise samples at the $N$ receive antennas, with average power $P_{noise} = E[|w_p|^2]$. With these notations, the expression of the vector $b$ of the $N$ received complex data symbols is given by:

$$b = \Gamma a + Qw; \qquad (1)$$

where, $\Gamma$ is the equivalent channel defined by:

$$\Gamma = QHP . \qquad (2)$$

### B. Performance metrics

Based on the diffraction theory, we expect the performance to increase with the following "physical metric" $m$:

$$m = \frac{R^2}{\lambda D}, \qquad (3)$$

where, $R$ is the radius of the circular array or half of the length of the linear array, $\lambda$ is the wavelength and $D$ is the transmitter-receiver distance. In fact, $m$ is simply proportional to the ratio of the transmit array maximum angular separation $A/D$ (i.e. the angle between the two antennas located at the array borders, thus separated by $A$, and viewed from a distance $D$ [9]) over the receive array maximum resolution $\lambda/A$ (i.e. the smallest angle between two objects that the receiver is able to resolve with an aperture $A$ [9]), where $A$ is the common aperture of the transmitter and the receiver (with $A = 2R$). We expect that a scheme (either SVD, DFT-SM or DFT-SM-MRT) tested with the same number of antennas and the same value of $m$ but with different combinations of $R$, $D$ and $\lambda$ values, and therefore different values of inter-antenna spacing, may result in a similar performance.
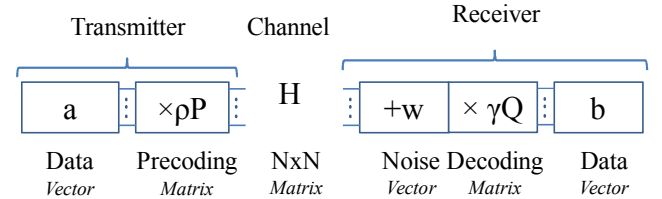


Fig. 4. System model

All the following performance metrics (defined hereafter) will be assessed as a function of the physical metric $m$: the SINR $x_n$ and the spectral efficiency $\Phi_n$ of data stream $n$ and the number of active data streams $N_a$. The data symbols and the noise samples are considered to be independent Gaussian variables with zero mean. The same assumption is taken for the interference which is supposed to be a large sum of independent variables. With these assumptions, and based on (1), one can derive the following SINR expression for $x_n$:

$$x_n = \frac{|\Gamma_{nn}|^2 P_{data}}{P_{noise} + \sum_{q=0,q\neq n}^{N-1}|\Gamma_{nq}|^2 P_{data}} \qquad (4)$$

Per sub-carrier and per data stream Adaptive modulation and coding (AMC) is assumed. $\varphi_{min}$ and $\varphi_{max}$ are the minimum and maximum spectral efficiencies, achievable with practical modulation and coding schemes (MCS). We set $\varphi_n = \log_2(1 + x_n)$ . The expression of $\Phi_n$ is given by: $\Phi_n = \varphi_n$ if $\varphi_{min} \leq \varphi_n \leq \varphi_{max}$ , $\Phi_n = 0$ if $\varphi_n < \varphi_{min}$ , and $\Phi_n = \varphi_{max}$ if $\varphi_n > \varphi_{max}$.

If $\Phi_n = 0$, the stream $n$ is considered 'inactive', if $\Phi_n > 0$, the stream $n$ is considered 'active'. $N_a$ is the number of active streams. The inactive streams are sent, consuming power and creating interference. This is sub-optimal, of course. Ideally, a reduced and optimum set of data streams (after an exhaustive search over all possible combinations of streams) would be selected, at the cost of extra complexity. However, the main objective of the study is to see the potential benefit of the precoders/decoders alone, without smart power allocation and stream selection.

## III. STUDIED SYSTEMS

This section presents the specific expressions of the P, Q and $\Gamma$ matrices introduced in section II for the SVD, DFT-SM, DFT-SM-MRT and "DFT-SM-MRT filtered" schemes. We here define the matrix M by: $M = H(H)^H$. We recall that the expression of the MRT precoder is $H^H$ [12].

### A. SVD

In the studied SVD scheme, the data stream $n$ is mapped onto the $n^{th}$ singular value of M. The SVD of M is given by $M = U\Delta V$, where U and V are unitary matrices and $\Delta$ is a diagonal matrix with the singular values as coefficients. The expressions of P, Q and $\Gamma$ are given by: $P = H^H V^H$; $Q = U^H$ and $\Gamma = \rho\gamma\Delta$ . H is a square matrix, therefore one could simply make the SVD of H and use the following equality to simplify the system: $V = U^H$. However, we prefer to study the SVD of M, as it has the advantage to be applicable to non-square MIMO matrices.

### B. DFT-SM

The expressions of P, Q and $\Gamma$ are given by: $P = A^{IDFT}$; $Q = A^{DFT}$ and $\Gamma = \rho\gamma A^{IDFT} H A^{DFT}$ .

### C. DFT-SM-MRT

The expressions of P and Q and $\Gamma$ are therefore given by: $P = H^H A^{IDFT}$; $Q = A^{DFT}$ and $\Gamma = \rho\gamma A^{DFT} M A^{IDFT}$ .

### D. DFT-SM-MRT filtered

In the "DFT-SM-MRT filtered" scheme, the system computes the expected spectral efficiency for the DFT-SM-MRT in a first step. Then, it determines which streams are not useful to be transmitted (inactive streams), and thus only transmits the other streams (active streams). In this case, the model presented in II must be slightly modified: $a$ , P , Q and $\Gamma$ are replaced by $a'$ of size $N_a$, with $E[\frac{1}{N_a}\sum_{n=0}^{N_a-1}|'a_n|^2]$, P' of size $N \times N_a$, Q' of size $N_a \times N$ and $\Gamma'$ of size $N_a \times N_a$. P' and Q' only include the lines of P and the column of Q, respectively, which correspond to active streams and $\Gamma' = Q'HP'$. The SINR expression $x'_n$ is then computed using (4), with $\Gamma'$ and $N_a$ instead of $\Gamma$ and $N$, and for active streams only. Finally, $\Phi_n$ is updated with $x'_n$ instead of $x_n$, using the same

method as in (II-A). This scheme suppresses the interference created by inactive streams over active streams, by simply muting inactive streams. We do not propose filtering for SVD as it is already orthogonal. We do not propose it for DFT-SM either, as it is expected to deliver almost no active data streams in the misalignment conditions [18,19].

### E. Basic Complexity Comparison

This section gives a first complexity analysis of the studied schemes, for large values of the number $N$ of antennas.

First of all, the complexity at the transmitter side is estimated. MRT needs a matrix transposition, a matrix conjugation and a matrix multiplication. Compared to MRT, DFT-SM-MRT requires an additional DFT. Compared to MRT, the studied SVD scheme needs an additional SVD. According to [21,22], the complexity of the FFT scales with $\Lambda_1(N) = N\log_2(N)$, and the complexity of SVD scales with $\Lambda_2(N) = N^3$. We define the complexity ratio $\Lambda(N)$ between the SVD and the DFT-SM-MRT schemes as: $\Lambda(N) = \frac{\Lambda_2(N)}{\Lambda_1(N)} = \frac{N^2}{\log_2(N)}$. Fig. 1 plots $\Lambda(N)$ as a function of the number of antennas $N$, and shows that $\Lambda(N)$ becomes tremendous for large MIMO systems ($N > 100$).

Now, on the receiver side, MRT needs no particular operation. DFT-SM-MRT and SVD schemes need the same operations as for the transmitter side, and therefore have the same complexity ratio.
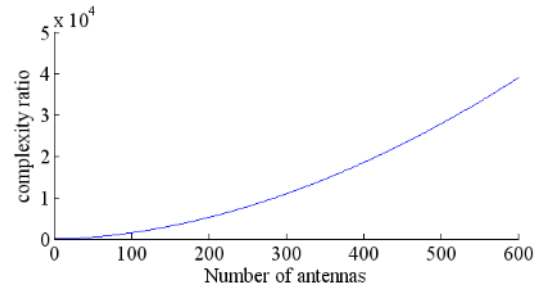


Fig. 5. Complexity ratio versus number of antennas

To conclude, at first sight, SVD is much more complex than DFT-SM-MRT especially for large MIMO systems. Computations based on low complexity implementations of the SVD would be needed for a more fair comparison.

## IV. PERFORMANCE EVALUATION METHODOLOGY

### A. Main assumptions

The number of antennas $N$ is fixed to 512.

The system carrier frequency $f$ is varied. The wavelength $\lambda$ is given by: $\lambda = c/f$, where $c$ is the speed of light.

Regarding the MCS, quadrature phase shift keying (QPSK) with coding rate ½ is chosen as the lowest MCS, corresponding to $\varphi_{min} = 1$ bits/s/Hz, and 64 Quadrature Amplitude Modulation (QAM) with coding rate 1 is chosen as the maximum MCS, corresponding to $\varphi_{max} = 6$ bits/s/Hz.

As we are considering a single carrier transmission, the value of the power spectral density (in watts per Hz, or watts × seconds) is used instead of the power (in watts) for $P_{data}$ and $P_{noise}$. $P_{data}$ is chosen equal to $20\text{dBm} \times T_{symbol}$, with $T_{symbol} = 800$ ns, which corresponds to a typical value for 60GHz standards [1-3] and $P_{noise} = F_i N_o$, where $N_o$ is the thermal noise power spectral density and $F_i$ is the noise figure. $N_o = -174\text{dBm/Hz}$ and $Fi = 5\text{dB}$.

### B. Misaligned arrays

As already stated in II, the transmit antenna array and the receive antenna array are identical, and have $N$ elements. Linear arrays of lengths $2R$ and circular arrays of radius $R$ are tested, to ensure they have the same aperture: $A = 2R$. The positions of the transmitter and the receiver arrays are determined using a two step approach. In a first step, they are "aligned": i.e. they are set perpendicular to the y-axis, centered over the y-axis and separated by the distance D. In the linear case, the arrays are set parallel to the z-axis. In a second step, a translation by $\delta_z$ along the z-axis is applied to the receive array, and rotations by the angles $\vartheta_x$, $\vartheta_y$ and $\vartheta_z$ around the x-axis, y-axis and z-axis, respectively, are applied to the transmit array. Circular and linear arrays are illustrated in Fig. 6 and Fig. 7 respectively.
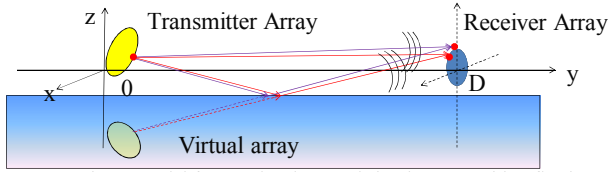


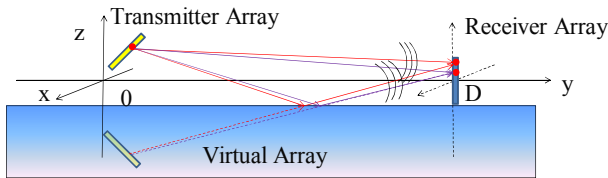Fig. 6. Model for translated, rotated circular array with reflection



Fig. 7. Model for translated, rotated linear array with reflection

### C. Channel Model

The MIMO channel H is generated using a ray tracing propagation model. One infinite and perfectly flat reflector (illustrated by Fig. 6 and Fig. 7) is considered. It is orthogonal to the z-axis and its coordinate is: $z = -R$. A virtual source, defined as the symmetrical image of the array through the surface, is used to model the perfect reflection. This could be, for instance, a basic model for a roof top. A reflection coefficient $r$ is applied. The path loss between the transmit antenna $n$ and the receive antenna $q$ is given by [4-6]:

$$g(\delta_{nq}) = \left(\frac{\lambda}{4\pi\delta_{nq}}\right)^2 10^{-0.1 \times \alpha \times \left(\frac{\delta_{nq}}{1000}\right)} ;$$

where $\alpha$ is the oxygen loss, $\delta_{nq}$ is the distance between the transmit antenna $q$ and the receive antenna $n$. Let $\delta'_{nq}$ be the distance between the virtual source corresponding to the reflection of antenna $q$ and the receive antenna $n$. The same

equation can be used with $\delta'_{nq}$ instead of $\delta_{nq}$. The channel coefficient $H_{nq}$ is therefore:

$$\text{H}_{nq} = \sqrt{g(\delta_{nq})}e^{j2\pi\frac{\delta_{nq}}{\lambda}} + r\sqrt{g(\delta'_{nq})}e^{j2\pi\frac{\delta'_{nq}}{\lambda}} .$$

### D. Testing various configurations

In order to make the study with arbitrary inter-antenna spacings (with respect to the transmitter-receiver distance, and the wavelength), all possible combinations of the following values for the frequency, the radius and the transmitter-receiver distance, are tested: $f$ between 10 and 100GHz; R between 0.4 and 3 meters and D between 10 and 100 meters.

For each combination, the physical parameter $m$ is computed using (3) and the metrics $\text{N}_a$ and $\Phi_n$ are computed using the equations in section II and the matrices defined in III.

All possible combinations of the following values for the rotation, the translation and the reflection are tested: $\vartheta_x$, $\vartheta_y$ and $\vartheta_z$ between 0 and 0.2 radians (~11°), $\delta_z$ between 0 and 20cm, $r = 0$ (no reflection) or $r = 1$ (reflection).

## V. RESULTS

All simulation results are plotted as a function of the physical parameter $m$, with values between 0 and 40. Points with $m$ beyond 40 correspond to huge arrays being very close to each other, compared to the wavelength. Such configurations are likely to be more rare than configurations with $m < 40$. Also, in those configurations, the SVD performance saturates due to the fixed number of antennas $N = 512$. In other terms, the channel becomes close to full rank, and low complexity precoders or decoders such as ZF, MMSE or even MRT may suffice. Here are two examples of scenarios corresponding to $m = 40$: $R = 3\text{m}$, $D = 45\text{m}$ and $f = 60\text{GHz}$, or $R = 3\text{m}$, $D = 75\text{m}$ and $f = 100\text{GHz}$.
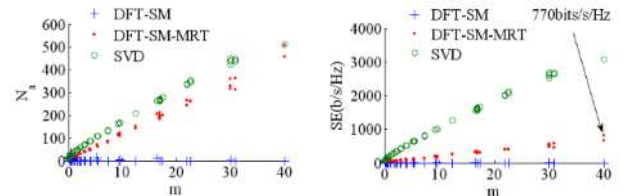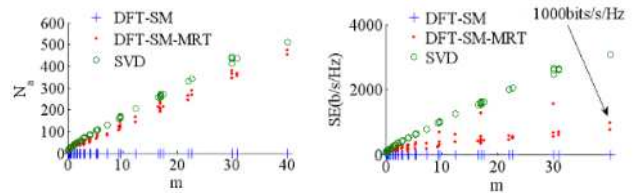


Fig. 8. Circular array, translation effect only



Fig. 9. Circular array, rotation effect only

Fig. 8 illustrates the number of active streams $N_a$ and the spectral efficiency $\Phi_n$ as a function of the physical parameter $m$, for SVD, DFT-SM and DFT-SM-MRT, when only translation is activated ($\vartheta_x = \vartheta_y = \vartheta_z = r = 0$, and $\delta_z \geq 0$). Fig. 9 illustrates the impact of rotation alone, ($\delta_z = r = 0$, $\vartheta_x \geq 0$, $\vartheta_y \geq 0$, and $\vartheta_z \geq 0$). As expected, for all schemes, the

performance mainly depends on $m$. One can observe that DFT-SM fails to deliver active streams due to the slight misalignment induced by either the translation or the rotation, whereas DFT-SM-MRT delivers almost the same number of active streams as SVD. Regarding the spectral efficiency, DFT-SM-MRT reaches around one third of the SVD performance.
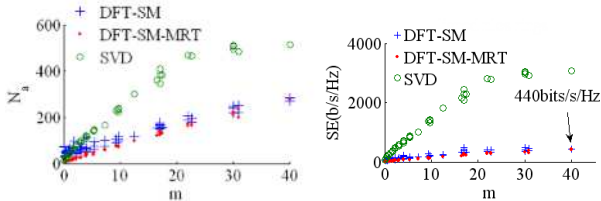


Fig. 10. Circular array, reflection effect only

Fig. 10 illustrates the impact of the reflector alone, ($\vartheta_x = \vartheta_y = \vartheta_z = \delta_z = 0$, and $r = 1$). This time, the transmitter and the receiver are perfectly aligned, and one reflector creates an additional path in the propagation channel. DFT-SM alone is already robust to the multi-path, and DFT-SM-MRT does not bring additional gain, because the alignment is already perfect.
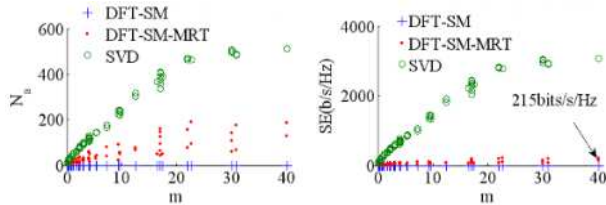


Fig. 11. Circular array, rotation, translation and reflection effects

Fig. 11 illustrates the combined effect of misalignment and reflection. Again, due to the misalignment, and contrary to DFT-SM-MRT, DFT-SM performance collapses.
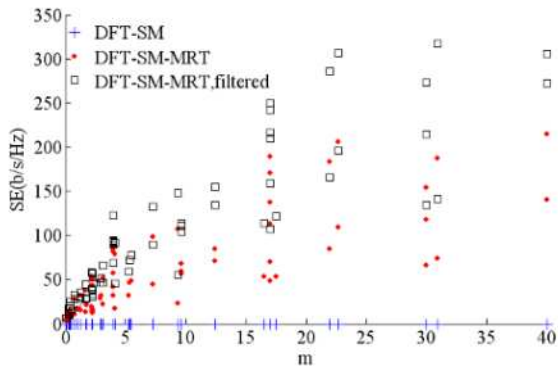


Fig. 12. Circular array, rotation, translation and reflection (Zoom)

Fig. 12 is a zoom of Fig. 11 with "DFT-SM-MRT filtered" scheme added. The filtered scheme, slightly improves the performance by muting non active streams, and by reducing the level of interference over active streams. We recall that filtering is not proposed for SVD which is already orthogonal. It is not implemented for DFT-SM either, due to the very low number of active data streams.

The same analysis as was shown from Fig. 8 to Fig. 12, can be made for the linear case, with Fig. 13 to Fig. 17. However,

the linear array is much more sensitive to rotation than to translation. Also, when comparing Fig. 12 and Fig. 17, one can observe that the circular array outperforms the linear array for the same value of the physical parameter. Hence, even though DFT-SM-MRT adapts to m as SVD does, without requiring an optimised antenna spacing with respect to m, it still clearly needs some particular antenna array "shapes".
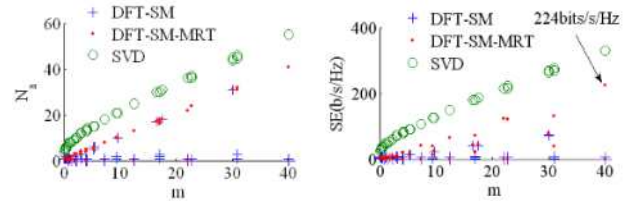


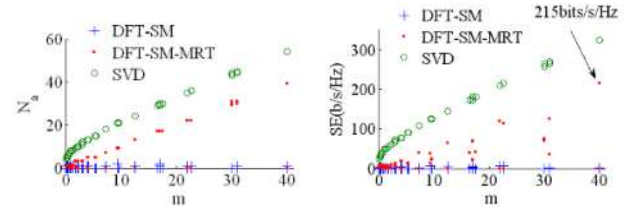Fig. 13. Linear array, translation effect only
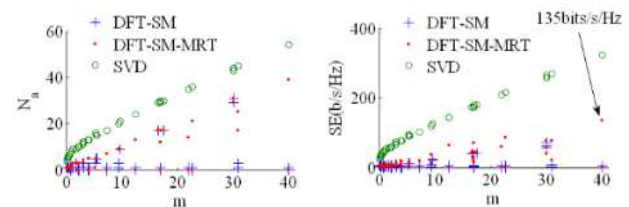


Fig. 14. Linear array, rotation effect only



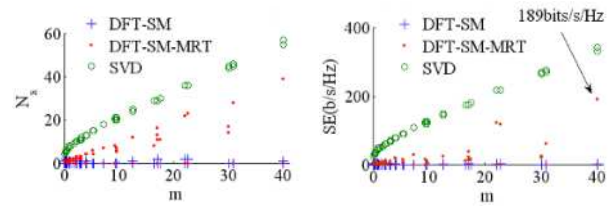Fig. 15. Linear array, reflection effect only



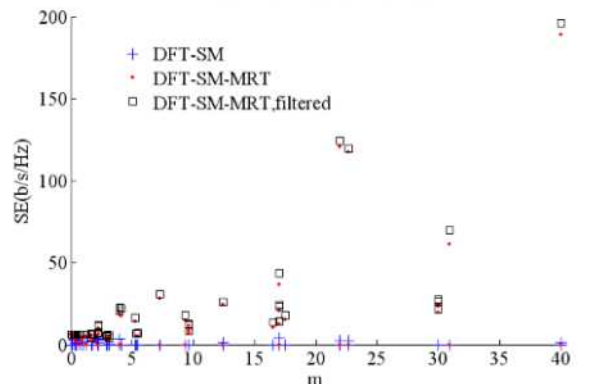Fig. 16. Linear array, translation, rotation and reflection effects



Fig. 17. Linear array, translation, rotation and reflection effects (Zoom)

Table I. summarizes the spectral efficiencies achieved by DFT-SM-MRT at $m$=40. Depending on the scenario, DFT-SM-MRT achieves hundreds of bits/s/Hz. In comparison with SVD, DFT-SMR-MRT achieves 1/3 to 1/14 of SVD performance, with a complexity which is around $\Lambda(N)^{-1} = 3.10^{-5}$ times lower, for the considered number of antennas (N=512).

TABLE I.        DFT-SM-MRT PERFORMANCE AT $m$=40

| Effects | DFT-SM-MRT spectral efficiency (bits/s/Hz) | | Ratio between DFT-SM-MRT and SVD spectral efficiencies | |
|---|---|---|---|---|
| | Circular Array | Linear Array | Circular Array | Linear Array |
| Translation | 770 | 224 | >1/3 | ~3/4 |
| Rotation | 1000 | 215 | ~1/3 | ~5/7 |
| Reflection | 440 | 135 | >1/7 | ~4/9 |
| All | 215 | 189 | >1/14 | ~5/8 |

To conclude this section, DFT-SM-MRT provides high spectral efficiency without inter-antenna spacing optimization with respect to the distance, and is robust to misalignement plus one reflector.

## VI. CONCLUSION

This paper introduces a new low complexity scheme for large MIMO millimeter-wave communications where the MIMO matrix is likely to be ill conditioned if the antenna separation is not optimized as a function of the transmitter-receiver distance. The proposed scheme, called DFT based spatial multiplexing with maximum ratio transmission, combines IDFT and maximum ratio transmission precoders at the transmitter and DFT decoder at the receiver. At first sight, the system has a much lower complexity than singular value decomposition, which is the chosen reference solution for ill conditioned MIMO. Simulations with a simple ray tracing model and one perfectly flat reflector show that the proposed scheme achieves a very high spectral efficiency and is robust to slight misalignment. Also it has been shown that the circular array outperforms the linear array. Future work will therefore focus on performance assessment with more realistic propagation channel models, on the design of new arrays shapes, and on some more precise complexity analysis.

## AKNOWLEDGEMENTS

## REFERENCES

[1] Giannetti , F. ; Luise, M. and Reggiannini , R., "Mobile and personal communications in the 60 GHz band: A survey," *Wireless Pers. Commun.*,vol. 10, no. 2, pp. 207–243, Jul. 1999.

[2] Wireless LAN Medium Access Control (MAC) and Physical Layer (PHY). Specification, IEEE Standard, Supplement to Standard 802 Part 11: Wireless LAN, New York, NY, 1999.

[3] Choi , C.-S.; Grass , E.; Piz, M.; Ehrig, M.; Marinkovic, M.; Kraemer, R. and Scheytt , C., "60-GHz OFDM systems for multi-gigabit wireless LAN applications", *IEEE CCNC 2010*.

[4] Mudumbai, R.; Singh, S.; Madhow, U.; "Medium Access Control for 60 GHz Outdoor Mesh Networks with Highly Directional Links," *INFOCOM 2009, IEEE* , vol., no., pp.2871-2875, 19-25 April 2009.

[5] Singh, S.; Mudumbai, R.; Madhow, U.; "Interference Analysis for Highly Directional 60-GHz Mesh Networks: The Case for Rethinking Medium Access Control," *IEEE/ACM Transactions on Networking,* vol.19, no.5, pp.1513-1527, Oct. 2011.

[6] Singh, S.; Mudumbai, R.; Madhow, U.; "Distributed Coordination with Deaf Neighbors: Efficient Medium Access for 60 GHz Mesh Networks," *Proc. IEEE INFOCOM*, vol., no., pp.1-9, 14-19 March 2010.

[7] Rappaport, T.S.; Shu Sun; Mayzus, R.; Hang Zhao; Azar, Y.; Wang, K.; Wong, G.N.; Schulz, J.K.; Samimi, M.; Gutierrez, F., "Millimeter Wave Mobile Communications for 5G Cellular: It Will Work!," Access, IEEE vol.1, no., pp.335,349, 2013.

[8] Gesbert, D.; Shafi, M.; Da-shan Shiu; Smith, P.J.; Naguib, A.; "From theory to practice: an overview of MIMO space-time coded wireless systems," *IEEE Journal on Selected Areas in Communications*, vol.21, no.3, pp. 281- 302, April 2003.

[9] Sheldon, C.; Torkildson, E.; Munkyo Seo; Yue, C.P.; Rodwell, M.; Madhow, U., "Spatial multiplexing over a line-of-sight millimeter-wave MIMO link: A two-channel hardware demonstration at 1.2Gbps over 41m range," *Wireless Technology, 2008. EuWiT 2008. European Conference on* , vol., no., pp.198,201, 27-28 Oct. 2008.

[10] Yoo, T. and Goldsmith , A., "Optimality of zero-forcing beamforming with multiuser diversity," *in Proc. IEEE ICC*, pp.542-546, May 2005.

[11] Sampath, H.; Stoica , P.; and Paulraj, A. J., "Generalized linear precoder and decoder design for MIMO channels using the weighted MMSE criterion," *IEEE Transactions on Communications,* vol.49, no.12, pp.2198–2206, Dec.2001.

[12] Lo, T. K Y, "Maximum ratio transmission," *Communications, IEEE Transactions on* , vol.47, no.10, pp.1458,1461, Oct 1999.

[13] Jeng-Shiann Jiang; Ingram, M.-A., "Spherical-wave model for short-range MIMO," *IEEE Transactions Communications*, vol.53, no.9, pp.1534,1541, Sept. 2005.

[14] Yang, H.; Marzetta, T.L., "Performance of Conjugate and Zero-Forcing Beamforming in Large-Scale Antenna Systems," *IEEE Journal on Selected Areas in Communications,* , vol.31, no.2, pp.172, Feb. 2013.

[15] Raja, M.; Muthuchidambaranathan, P.; "BER performance of SVD-based transmit beamforming with various modulation techniques," *Proc. 2010 International Conference on Industrial and Information Systems (ICIIS),* , vol., no., pp.155-160, July 29 2010-Aug. 1 2010.

[16] Feng Wang; Xia Liu; Bialkowski, M.E.; "Investigation into SVD Based Beamforming over Rician MIMO Channels," *in proc. WiCom '09. 5th International Conference on Wireless Communications, Networking and Mobile Computing, 2009.* , vol., no., pp.1-4, 24-26 Sept. 2009.

[17] Kohno, R.; Choonsik Yim; Imai, H., "Array Antenna Beamforming Based On Estimation Of Arrival Angles Using DFT On Spatial Domain," *IEEE International Symposium on Personal, Indoor and Mobile Radio Communications.* , vol., no., pp.38,43, 23-25 Sep 1991.

[18] Yang, D.; Yang, L.-L.; Hanzo, L., "DFT-Based Beamforming Weight-Vector Codebook Design for Spatially Correlated Channels in the Unitary Precoding Aided Multiuser Downlink" *in Proc. IEEE Int. Conf. Comm. 2010*, vol., no., pp.1,5, 23-27 May 2010.

[19] Edfors, O.; Johansson, A.J., "Is Orbital Angular Momentum (OAM) Based Radio Communication an Unexploited Area?," *IEEE Trans. on Antennas and Propagation* , vol.60, no.2, pp.1126,1131, Feb. 2012.

[20] Irmer, R.; Droste, H.; Marsch, P.; Grieger, M.; Fettweis, G.; Brueck, S.; Mayer, H.-P.; Thiele, L.; Jungnickel, V.; "Coordinated multipoint: Concepts, performance, and field trial results," *IEEE Communications Magazine,* , vol.49, no.2, pp.102-111, February 2011.

[21] Duhamel, P. and Vetterli, M., 1990, "Fast Fourier transforms: a tutorial review and a state of the art", Signal Processing 19: 259–299.

[22] Golub, G. H.; Van Loan, C. F. (1996). "Matrix Computations" (3rd ed.). Hopkins, J.